Icy Bodies of the Solar System
Proceedings IAU Symposium No. 263, 2009
J.A. Fernández, D. Lazzaro, D. Prialnik & R. Schulz, eds.

doi:10.1017/S1743921310002000

Deep Impact ejection from Comet 9P/Tempel 1 as a triggered outburst

Sergei I. Ipatov[1] **and Michael F. A'Hearn**[2]

[1]Catholic University of America
Washington DC, USA
email: siipatov@hotmail.com

[2]Dept. of Astronomy, University of Maryland,
College Park, MD, USA
email: ma@astro.umd.edu

Abstract. Ejection of material after the Deep Impact collision with Comet Tempel 1 was studied based on analysis of the images made by the Deep Impact cameras during the first 13 minutes after impact. Analysis of the images shows that there was a local maximum of the rate of ejection at time of ejection ∼10 s with typical velocities ∼100 m/s. At the same time, a considerable excessive ejection in a few directions began, the direction to the brightest pixel changed by ∼50°, and there was a local increase of brightness of the brightest pixel. The ejection can be considered as a superposition of the normal ejection and the longer triggered outburst.

Keywords. comets: general; solar system: general

1. Analysis of images

In 2005 the Deep Impact (DI) impactor collided with Comet 9P/Tempel 1 (A'Hearn *et al.* 2005). Our studies (Ipatov & A'Hearn 2008, 2009) of the time variations in the projections v_p of characteristic velocities of ejected material onto the plane perpendicular to the line of sight and of the relative rate r_{te} of ejection were based on analysis of the images made by the DI cameras during the first 13 min after the impact. We studied velocities of the particles that were the main contributors to the brightness of the cloud of ejected material, that is, mainly particles with diameter $d < 3$ μm. Below we present a short description of analysis of the images and the conclusions based on our studies. Details of the studies and more figures and references are presented in Ipatov & A'Hearn (2008). More complicated models of ejection will be studied in future.

Several series of images taken through a clear filter were analyzed. In each series, the total integration time and the number of pixels in an image were the same. As in other DI papers, original images were rotated by 90° in anti-clockwise direction. In DI images, calibrated physical surface brightness (hereafter CPSB, always in W m^{-2} sterad^{-1} micron^{-1}) is presented. For several series, we considered the differences in brightness between images made after impact and a corresponding image made just before impact. Overlapping of considered time intervals for different series of images allowed us to calculate the relative brightness at different times t after impact, though because of non-ideal calibration, the values of peak brightness at almost the same time could be different (up to the factor of 1.6) for different series of images. Variation in brightness of the brightest pixel and the direction from the place of ejection to the brightest pixel were studied. At t>100 s, some DI images do not allow one to find accurately the relative brightness of the brightest pixel and the direction from the place of ejection to this pixel. First, there are large regions of saturated pixels on DI images, which may not allow one to calculate

accurately the peak brightness. Secondly, at $t \sim 600 - -800$ s, coordinates of the brightest pixel were exactly the same for several images. It can mean that some pixels became 'hot' when the distance between the spacecraft and the nucleus of the comet became small.

We analyzed the time dependencies of the distances L from the place of ejection to contours of CPSB = const for several levels of brightness and different series of images (Fig. 1). Based on the supposition that the same moving particles corresponded to different local maxima (or minima) of $L(t)$ (e.g., to values L_1 and L_2 on images made at times t_1 and t_2), we calculated the characteristic velocities $v = (L_1\text{-}L_2)/(t_1\text{-}t_2)$ at time of ejection $t_e = t_1\text{-}L_1/v$. In this case, we use results of studies of series of images in order to obtain one pair of v_p and t_e. Such approach to calculations of velocities doesn't take into account that particles ejected at the same time could have different velocities. According to theoretical studies presented by Housen *et al.* (1983), velocities of ejecta are proportional to $t_e^{-\alpha}$ (with α between 0.6 and 0.75), and the rate r_{te} of ejection is proportional to $t_e^{0.2}$ at α=0.6 and to $t_e^{-0.25}$ at $\alpha = 0.75$. Our estimates of the pairs of v_p and t_e were compared with the plots of $v_{expt} = v_p = c(t/0.26)^{-\alpha}$ at several pairs of α and c (0.26 was considered because the second ejection began mainly at $t_e \approx 0.26$ s). The comparison testifies in favor of mean values of $\alpha \sim 0.7$. Destruction and sublimation of particles and variation in their temperature could affect on the brightness of the DI cloud, but, in our opinion, don't affect considerably on our estimates of velocities and slightly change estimates of α.

For the edge of bright region (usually at CPSB=3), the values of $L = L_b$ in km at approximately the same time can be different for different series of DI images considered. Therefore, we cannot simply compare L_b for different images, but need to calculate the relative characteristic size L_r of the bright region, which compensates non-ideal calibration of images and characterizes the size of the bright region. Considering that the time needed for particles to travel a distance L_r is equal to $dt = L_r/v_{expt}$, we find the time $t_e = t - dt$ of ejection of material of the contour of the bright region considered at time t.

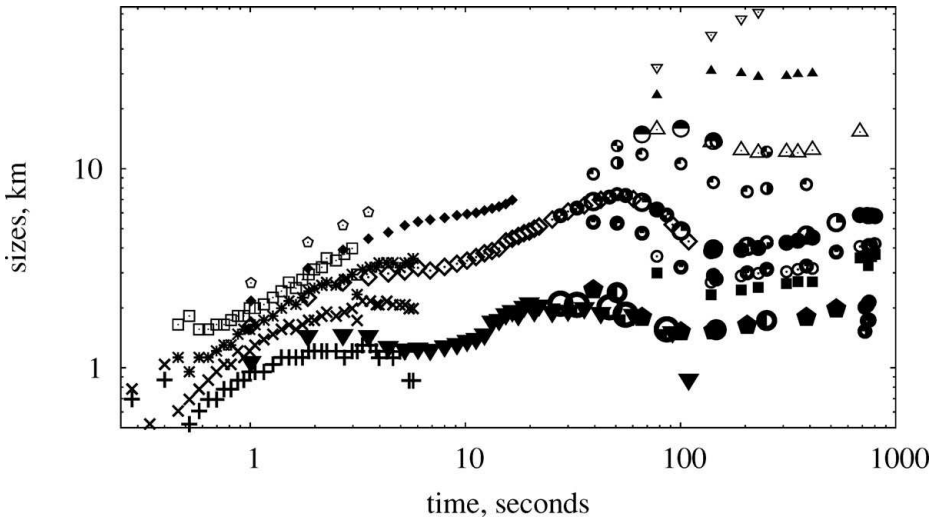

Figure 1. Time variations in sizes L (in km) of regions inside contours of CPSB=C. Different signs correspond to different series of images at different C. The curves have local minima and maxima that were used for analysis of time variations in velocities.

The volume V_{ol} of a spherical shell of radius L_r and width h is proportional to $L_r^2 h$, and the number of particles per unit of volume is proportional to $r_{te} \cdot (V_{ol} \cdot v)^{-1}$, where v is the velocity of the material. Here r_{te} corresponds to the material that was ejected at t_e and reached the shell with L_r at time t. The number of particles on a line of sight, and so the brightness B_r, are approximately proportional to the number of particles per unit of volume multiplied by the length of the segment of the line of sight inside the DI cloud, which is proportional to L_r. Actually, the line of sight crosses many shells characterized by different r_{te}, but as a first approximation we supposed that $B_r \propto r_{te}(v \cdot L_r)^{-1}$. For the edge of the bright region, $B_r \approx$ const. Considering $v = v_{expt}$, we calculated the relative rate of ejection as $r_{te}{=}L_r t^{-\alpha}$. Based on this dependence of r_{te} on time t and on the obtained relationship between t and t_e, we constructed the plots of dependences of r_{te} on t_e (Fig. 2). Because of high temperature and brightness of ejecta, the real values of r_{te} at $t_e < 1$ s are smaller than those in Fig. 2. As typical sizes of ejected particles increased with t_e, the real rate of ejection decreased more slowly than the plot in this figure. If, due to the outburst, typical velocities of observed ejected particles did not decrease much at $t_e > 100$ s, then the values of r_{te} could be greater than those in Fig. 2.

Excessive ejection in several directions ('rays' of ejection) was studied based on analysis of the form of contours of constant brightness. Bumps of the contours considered by Ipatov & A'Hearn (2008) include the upper-right bump ($\psi \sim 60 - 80°$, still seen at $t \sim 13$ min), the right bump (ψ increased from 90° at $t \sim 4 - 8$ s to 110-120° at $t \sim 25 - 400$ s), the left bump ($\psi \sim 245 - 260°$), which transformed with time into the down-left bump ($\psi \sim 210 - 235°$), the upper bump (backward ejection, ψ varied from 0 to -25°, the bump consisted mainly of particles ejected after 80 s), where ψ is the angle between the upper direction and the direction to a bump measured in a clockwise direction. Together with hydrodynamics of the explosion, icy conglomerates of different sizes at different places of the ejected part of the comet could affect on the formation of the rays.

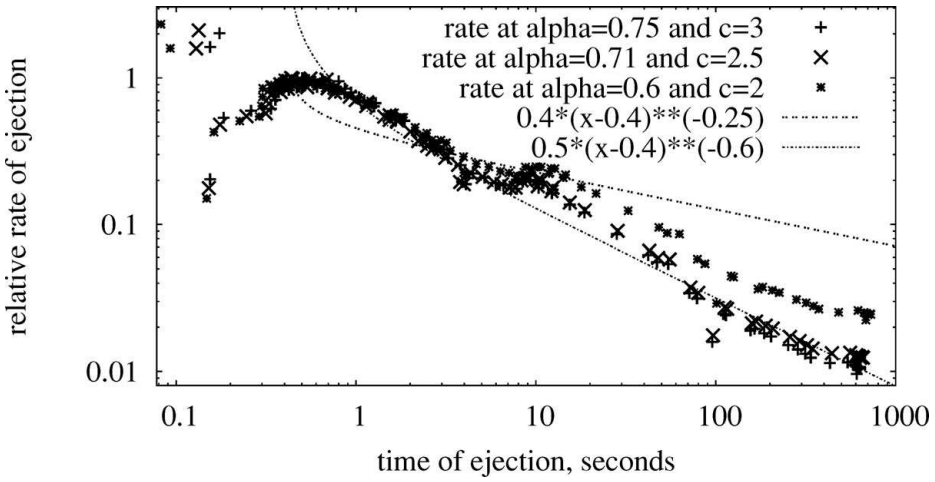

Figure 2. Relative rate r_{te} of ejection at different times t_e of ejection for the model in which the characteristic velocities of the edge of the observed bright region at time t are equal to $v_{expt}{=}c \cdot (t/0.26)^{-\alpha}$ (in km/s), for three pairs of α and c. The maximum rate at $t_e > 0.3$ s is considered to be equal to 1. Two curves of the type $y{=}c_r \cdot (x - c_t)^{\beta}$ are also presented for comparison.

2. Conclusions

Our studies showed that there was a local maximum of the rate of ejection at time of ejection $t_e \sim 10$ s (Fig. 2) with typical projections (onto the plane perpendicular to the line of sight) of velocities $v_p \sim 100 - -200$ m/s. At the same time, the considerable excessive ejection in a few directions (rays of ejecta) began, the direction to the brightest pixel quickly changed by about 50°, and there was a local increase of brightness of the brightest pixel. On images made during the first 10–12 s, the direction was mainly close to the direction of impact; after the jump, it gradually came closer to the direction of impact. These features at $t_e \sim 10$ s were not predicted by theoretical models of ejection and could be caused by the triggered outburst. At the outburst, the ejection could be from entire surface of the crater, while the normal ejection was mainly from its edges. Starting from 10 s, the ejection of more icy material could begin. The increase in the fraction of icy material caused an increase in the observed ejection rate and the initial velocities (compared to the normal ejection).

At $1 < t_e < 3$ s and $8 < t_e < 60$ s, the plot of time variation in estimated rate r_{te} of ejection of observed material was essentially greater than the exponential line connecting the values of r_{te} at 1 and 300 s. The difference could be mainly caused by that fact that the impact was a trigger of an outburst. The sharp decrease of the rate of ejection at $t_e \sim 60$ s could be caused by the decrease of the outburst and/or of the normal ejection. The contribution of the outburst to the brightness of the cloud could be considerable, but its contribution to the ejected mass could be relatively small. Duration of the outburst (up to 30–60 min) could be longer than that of the normal ejection (a few minutes). The studies testify in favor of a model close to gravity-dominated cratering.

Projections v_p of the velocities of most of the observed material ejected at $t_e \sim 0.2$ s were about 7 km/s. As the first approximation, the time variations in characteristic velocity at $1 < t_e < 100$ s can be considered to be proportional to $t_e^{-0.75}$ or $t_e^{-0.7}$, but they could differ from this exponential dependence. The fractions of observed small particles ejected (at $t_e \leqslant 6$ s and $t_e \leqslant 14$ s) with $v_p > 200$ m/s and $v_p > 100$ m/s were estimated to be about 0.13–0.15 and 0.22–0.25, respectively, if we consider only material observed during the first 13 min and $\alpha \sim 0.7 - -0.75$. These estimates are in accordance with the previous estimates (100–200 m/s) of the projection of the velocity of the leading edge of the DI dust cloud, based on various ground-based observations and observations made by space telescopes. The fraction of observed material ejected with velocities greater than 100 m/s was greater than the estimates based on experiments and theoretical models. Holsapple & Housen (2007) concluded that the increase of velocities was caused by vaporization of ice in the plume and by fast moving gas. In our opinion, the greater role in the increase of high-velocity ejecta could be played by the outburst (by the increase of ejection of bright particles), and it may be possible to consider the ejection as a superposition of the normal ejection and the longer triggered outburst. Time variations in velocities could be smaller (especially, at $t_e > 100$ s) for the outburst ejecta than for the normal ejecta.

The excess ejection of material in a few directions (rays of ejected material) was considerable during the first 100 s and was still observed in images at $t \sim 500 - -770$ s. The sharpest rays were caused by material ejected at ∼20 s. In particular, there were excessive ejections, especially in images at $t \sim 25 - -50$ s, in directions perpendicular to the direction of impact. Directions of excessive ejection could vary with time.

Acknowledgements

The work was supported by NASA DDAP grant NNX08AG25G.

References

A'Hearn, M. F. *et al.* 2005, *Science*, 310, 258
Holsapple, K. A. & Housen, K. R. 2007, *Icarus*, 187, 345
Housen, K. R., Schmidt, R. M., & Holsapple, K. A. 1983, *J. Geophys. Res.*, 88, 2485
Ipatov, S. I. & A'Hearn, M. F. 2008, *http://arxiv.org/abs/0810.1294*
Ipatov, S. I. & A'Hearn, M. F. 2009, *Lunar. Planet. Sci.* XL, 1022 (abstract)